JOURNAL OF MATERIALS SCIENCE **35** (2000) 5241–5246

X-ray diffraction study of polyphilic smectic liquid crystals

G. UNGAR*, K. NOBLE
Department of Engineering Materials, University of Sheffield, Sheffield S1 3JD, UK
E-mail: g.ungar@sheffield.ac.uk

V. PERCEC, G. JOHANSSON
Department of Chemistry, University of Pennsylvania, PA 19104-6323, USA

4-substituted *n*-5,5,6,6,7,7,8,8,9,9,10,10,10-tridecafluorodecan-1-yloxybenzene and *n*-5,5,6,6,7,7,8,8,9,9,10,10,11,11,12,12,12-pentadecafluorododecan-1-yloxybenzene, the former with CO_2CH_3 and the latter with CO_2CH_3 and CO_2H substituents in *para* position, are polyphilic compounds exhibiting smectic liquid crystalline phases. The structure of these phases was studied by X-ray diffraction and modelling. The method consisted of reconstructing all possible one-dimensional electron density profiles from diffraction intensities and matching them with the profiles calculated from structural models. The method is shown to be useful in both determining molecular arrangement in the smectic phase and in phase identification itself. An S_{Ad} phase is found in the two esters, having interdigitated perfluorinated alkyl segments. In contrast, a double-layer S_C phase, also known as S_{C2}, is found in the carboxylic acid. The method used here is particularly applicable to polyphilic liquid crystals such as the present ones, which are characterized by a complex electron density profile and a high translational order parameter.

1. Introduction

Amphiphilic character of molecules serves many useful purposes, being responsible for lyotropic properties of surfactants and lipids and, to a large extent, for thermotropic properties of low molar and polymeric liquid crystals and supramolecular self-assembled systems [1]. Polyphilic linear mesogens, containing several mutually incompatible segments, are considered, among other things, to be candidates for longitudinal ferroelectric liquid crystals [2, 3]. The latter are envisaged as smectics with spontaneous polarization parallel to the director i.e. normal or nearly normal to the smectic layers [4]. This is in contrast to the more conventional S_{C^*} ferroelectric liquid crystals where the net dipole is normal to the molecular axis and parallel to the layer planes [5, 6]. An example of how a longitudinal ferroelectric may be formed from tetraphilic linear molecules is shown in Fig. 1. Here a molecule consists of four segments where the preferred attractive interactions are B-B, C-C and A-D. This ensures that the low-energy ordered smectic structure is non-centrosymmetric. In order to allow effective switching the interactions must be weak [7].

In the present work we investigate smectic liquid crystals of polyphilic compounds containing perfluorinated, alkyl, aromatic and polar units. However, the conditions for longitudinal ferroelectricity are not met. Specifically, the condition that A-D interaction be stronger than A-A and D-D interactions is not fulfilled and the compounds indeed do not show spontaneous polarization [8]. Nevertheless, it is instructive to study the modes of packing of such polyphilic molecules within smectic layers in order to establish some general principles of self-assembly of polyphiles. We employ here a combination of molecular modelling and reconstruction of electron density profiles based on X-ray diffraction.

2. Materials and experimental method

Presently we investigate smectic liquid crystals of 4-substituted *n*-5,5,6,6,7,7,8,8,9,9,10,10,10-tridecafluorodecan-1-yloxybenzene and *n*-5,5,6,6,7,7,8,8,9,9,10,10,11,11,12,12,12-pentadecafluorododecan-1-yloxybenzene, the former with CO2CH3 and the latter with CO_2CH_3 and CO_2H substituents:

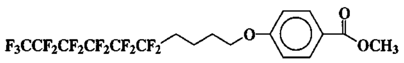

10F6CO$_2$CH$_3$

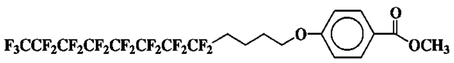

12F8CO$_2$CH$_3$

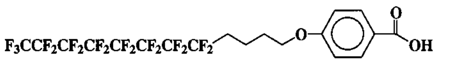

12F8CO$_2$H

---

* Author to whom all correspondence should be addressed.

0022–2461 © *2000 Kluwer Academic Publishers*

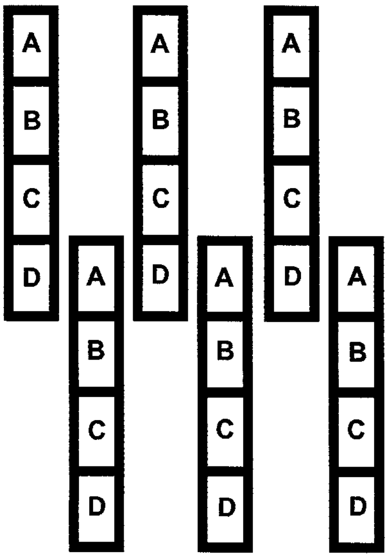

Figure 1 Schematic diagram of a layer of a longitudinal ferroelectric smectic liquid crystal consisting of tetraphilic molecules. Preferred interactions are B-B, C-C and A-D.

These mesogenic materials are of a somewhat non-standard type in that they contain only one benzene ring. The synthesis has been described elsewhere [9]. All these and some other related compounds were found to exhibit stable enantiotropic smectic phases [9]. Transition temperatures, as determined by a combination of DSC and polarised optical microscopy, are:

10F6CO2CH3: $k_1 \xrightarrow{44} k_2 \underset{17}{\overset{54}{\rightleftharpoons}} S \underset{52}{\overset{58}{\rightleftharpoons}} I$

12F8CO2CH3: $k \underset{52}{\overset{69}{\rightleftharpoons}} S \underset{75}{\overset{81}{\rightleftharpoons}} I$

12F8CO2H: $k_1 \underset{152}{\overset{165}{\rightleftharpoons}} k_2 \underset{173}{\overset{178}{\rightleftharpoons}} S \underset{189}{\overset{193}{\rightleftharpoons}} I$

The compounds could be described as tetraphilic. The blocks A, B, C and D (Fig. 1) are, respectively, the perfluorinated, alkyl, phenylene and ester/carboxylic moieties.

X-ray diffraction experiments were performed using a pinhole-collimated $\mathrm{Cu}_{K\alpha}$ beam and an image plate area detector (MarResearch). Powder specimens in thin-walled glass capillaries were held in a temperature cell controlled to ±0.5°C. Radial intensity scans $I(r)$ were obtained by azimuthal averaging:

$$I(r) = \frac{2\pi}{r} \int_0^{2\pi} I_{r,\alpha}(\alpha)\,\mathrm{d}\alpha$$

where α is the azimuthal angle. Macromodel software was used for molecular modelling and energy minimization and the output atomic coordinates were imported into custom programs for further processing.

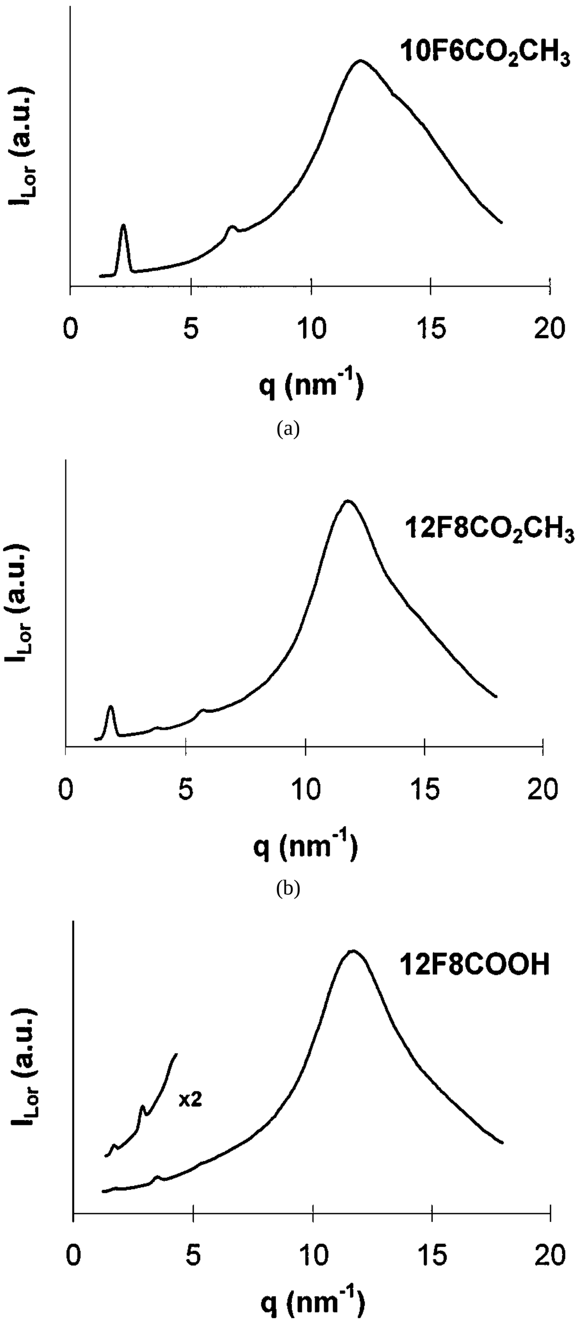

(a)

(b)

(c)

Figure 2 Powder diffractograms of compounds **10F6PhCO$_2$CH$_3$** (a), **12F8PhCO$_2$CH$_3$** (b) and **12F8PhCO$_2$H** (c) recorded in the temperature range of their smectic phase. Lorentz corrected intensities are shown *vs.* wavevector Q, where $Q = 4\pi(\sin\Theta)/\lambda$. The inset in (c) shows the lower-angle section with the intensities expanded by a factor of 2. Layer reflections correspond to the following spacing: (a) 2.82 nm, 0.94 nm; (b) 3.33 nm, 1.65 nm, 1.10 nm; (c) 3.63 nm, 1.81 nm, 1.19 nm.

3. Results

Fig. 2a–c, respectively, show powder diffractograms of compounds **10F6PhCO$_2$CH$_3$**, **12F8PhCO$_2$CH$_3$** and **12F8PhCO$_2$H**. Lorentz corrected intensities are shown *vs.* wavevector Q, where $Q = 4\pi(\sin\Theta)/\lambda$. The scattering function is dominated by a broad diffuse maximum in the Q region of 12 nm^{-1}, i.e. of real space interactions of the order of $2\pi/Q = 0.5$ nm. This shows that only short-range liquid-like positional order exists on the interatomic scale. The sharp peaks in the low-angle region have their Q-values in the ratio 1 :2 : 3 and are therefore indicative of smectic ordering. This is consistent with the focal conic textures observed by polarized optical microscopy [9]. Considering the lack of positional long range order in the $Q \geq 10$ nm^{-1} range, the choice

TABLE I X-ray diffraction data pertaining to the layer reflections of the smectic phase

Compound	T (°C)	Measured spacing L (nm)	Molecular length ℓ (nm)*	L/ℓ	Structure factors F_1	F_2	F_3
10F6PhCO$_2$CH$_3$	54	2.82	2.21	1.3	100	0	23
12F8PhCO$_2$CH$_3$	76	3.31	2.46	1.3	100	8	14
12F8PhCO$_2$H	187	3.60	2.30	1.6	36	100	50

*from molecular model

of phases is narrowed to S_A or possibly S_C. Table I lists the measured layer spacings L of the smectic phase for the three compounds, together with the lengths ℓ of extended molecules from model. L/ℓ ratios are 1.3 for the esters and 1.6 for the acid. Traditionally one would interpret this information as showing the partially interdigitated smectic-A phase, or S_{Ad}.

It is notable that in the case of the present ester compounds the intensities of the first and third orders, I_1 and I_3, are the highest (Fig. 2a and b); in **10F6PhCO$_2$CH$_3$** the second order is in fact completely absent. In contrast, in **12F8PhCO$_2$H** it is the second order which is the strongest (Fig. 2c). Situations where three diffraction orders have comparable intensities are generally rare in thermotropic smectic liquid crystals, where the first order is usually dominant and sometimes the only Bragg reflection observed. However, the occurrence of a number of intense higher orders is not uncommon in polyphilic liquid crystals, whether smectic, columnar or cubic [10, 11].

In order to utilise the information contained in the diffraction intensities we have taken an approach of generating a series of smectic layer models and their simulated 1-dimensional electron density distributions, and comparing the latter with all possible electron density profiles reconstructed from experimental diffraction intensity data. The best fit models are then accepted as the most likely structures.

As mentioned above, electric polarization experiments have established a lack of spontaneous polarization, hence the smectic layers are centro-symmetric. Consequently, for the purpose of calculating a model electron density distribution along the layer normal $\rho(x)_{i,X}$, a smectic layer can be represented by two molecules related by a 180° rotation around an in- layer axis [12]. The remaining degrees of freedom are molecular conformation i, which includes tilt of different sections of the molecule [13], and molecular displacement X along the layer normal $\underline{\mathbf{x}}$ [9, 14]. Representative two-molecule models are shown at the bottom of Figs 3–5 for compounds **10F6PhCO$_2$CH$_3$**, **12F8PhCO$_2$CH$_3$** and **12F8PhCO$_2$H**. The constraint imposed is that the period along $\underline{\mathbf{x}}$, i.e. the layer thickness, must be equal to L, the measured X-ray periodicity.

Electron density profile $\rho(x)_{i,X}$ for each model is approximated by a histogram with the $0 < x < L$ range divided into K discrete intervals (cells) Δx. For the k-th interval

$$\rho_k \Delta x = \sum_j Z_{j,k}$$

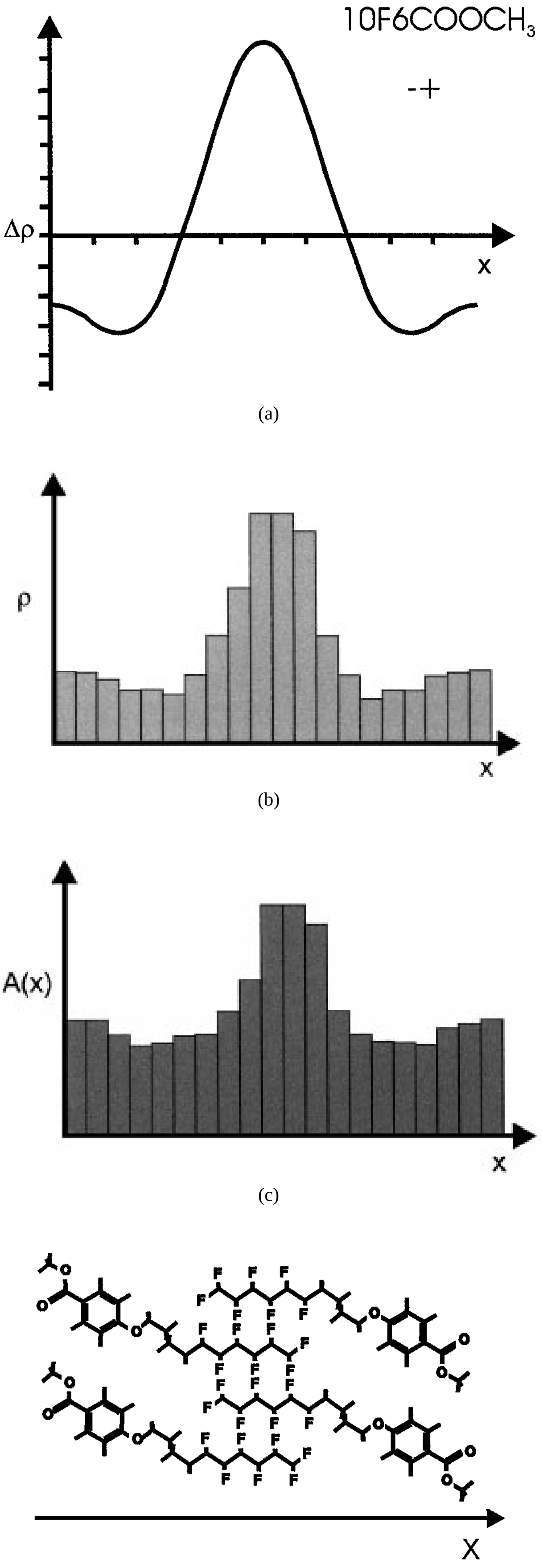

(a)

(b)

(c)

(d)

Figure 3 Composite diagram showing the best fit model structure of the smectic phase of **10F6PhCO$_2$CH$_3$** (d), the corresponding calculated cross-section profile $A(x)$ (c) and electron density profile $\rho(x)$ (b), and the electron density deviation from average, $\Delta\rho(x)$, reconstructed from the experimental diffraction intensities (a). The phase angle choice is indicated by the sequence of signs in (a) for the three (two) reflection orders. $\underline{\mathbf{x}}$ is normal to the layers. One layer period is shown ($0 < x < L$).

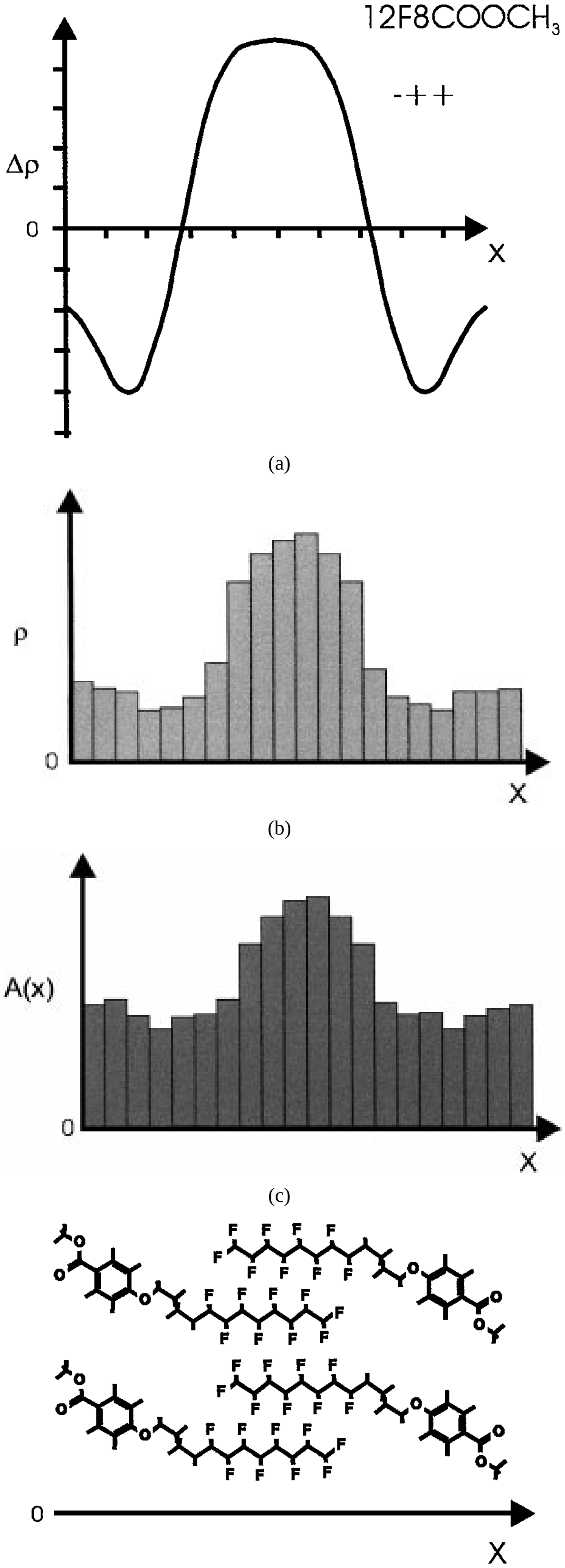

(a)

(b)

(c)

(d)

Figure 4 Same as Fig. 3 but for **12F8PhCO$_2$CH$_3$**.

where the summation is over all atoms within the interval, Z being the atomic number. The histogram $\rho(x)$ was further subjected to a three-cell smooth:

$$\rho'_k = \frac{1}{2}\left(\rho_k + \frac{\rho_{k-1} + \rho_{k+1}}{2}\right)$$

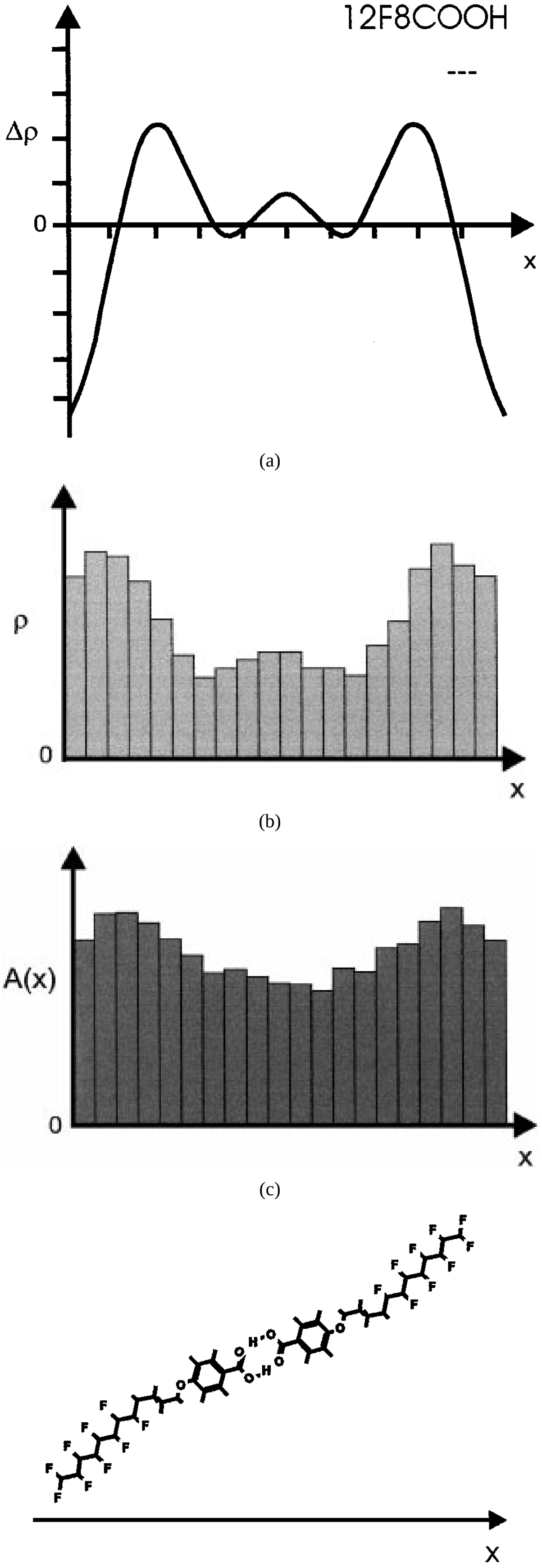

(a)

(b)

(c)

(d)

Figure 5 Same as Fig. 3 but for **12F8PhCO$_2$H**.

Periodic boundary condition $\rho_{K+k} = \rho_k$ applies. Electron density histograms obtained from the models in Figs 3d, 4d and 5d are shown in Figs 3b, 4b and 5b.

Layer models whose $\rho(x)$ profiles were to be compared with experimental data were additionally screened for viability in terms of space filling. This was accomplished by constructing a van der Waals cross-section profile $A(x)$ along $\underline{\mathbf{x}}$. This profile was also approximated by a histogram where

$$A_k \Delta x = \sum_j V_{j,k}^{\mathrm{corr}}$$

Here $V_{j,k}^{\mathrm{corr}}$ is the volume of j-th atom in k-th cell. $V_{j,k}^{\mathrm{corr}}$ is the van der Waals volume of the spherical atom corrected for the overlap with bonded atoms. $A(x)$ profiles of the models in Figs 3d, 4d and 5d are shown in Figs 3c, 4c and 5c.

Since the electron density profile of a smectic liquid crystal is a periodic function, it can be represented as a Fourier series. Since our liquid crystal has a centre of symmetry, the profile is an even function, i.e. $\rho(-x) = \rho(x)$. Hence ρ can be expanded in a cosine series:

$$\rho(x) = \sum_{n=0}^{\infty} F_n \cos\left(\frac{2\pi n x}{L}\right)$$

Coefficients F_n are amplitudes of X-ray diffraction orders n, related to corrected intensities by $I_n = F_n^2$. Since I_0 and A_0 are unobtainable, and

$$F_0 = \frac{1}{L} \int_0^L \rho(x)\,\mathrm{d}x$$

we can only aim at reconstructing the electron density deviation from the average value, i.e. $\Delta\rho(x) = \rho(x) - \langle\rho\rangle$:

$$\Delta\rho(x) = \sum_{n=1}^{N} F_n \cos\left(\frac{2\pi n x}{L}\right)$$

In the present work the summation is performed over the $N = 3$ visible diffraction orders.

The phase problem for a centrosymmetric structure reduces to the choice of sign of F_n. There are $2^N = 2^3 = 8$ $\Delta\rho(x)$ profiles reconstructible from $N = 3$ reflections. Four of those are negatives of the other four. Similarly, four profiles are obtainable from the other four by choosing the origin at $x = L/2$ instead at $x = 0$.

Experimental amplitudes F_n, obtained from corrected integral intensities of the three layer diffraction orders, are listed at the right hand side of Table I. Different models were examined for each compound, with different molecular conformations and shifts X, while maintaining L constant. A number of cases were rejected on grounds of the cross-section profile $A(x)$ being too uneven, which would result in unacceptably low packing density. The simulated electron density distributions $\rho(x)$ were compared with all eight "experimental" profiles $\Delta\rho(x)$ for each compound. $\Delta\rho(x)$ functions with pronounced maxima at the layer surfaces, i.e. at $x = 0$ and L, are deemed unlikely for a smectic liquid crystal.

The process of finding the best match between the different "experimental" and simulated electron density distributions resulted in the best fit structures shown, respectively, in Figs 3–5 for compounds **10F6Ph CO_2CH_3**, **12F8PhCO_2CH_3** and **12F8PhCO_2H**.

4. Discussion

In spite of the fact that layer spacings L of the three compounds are not too dissimilar, the packing of **12F8PhCO_2H** is fundamentally different from that of the esters. According to the models, molecules of the esters have their perfluorinated chain segments interdigitated (Figs 3 and 4), while the acid effectively forms a double-layer structure, free of interdigitation, but with the molecular axis tilted with respect to the layer normal (Fig. 5).

The overlap of the perfluorinated segments of ester molecules is understandable in terms of the polyphilic nature of the molecules and of dipolar interaction. It is worth noting that in the proposed structure the short alkoxy (propyloxy) segments are not interdigitated, although the cross-section of their extended conformation is slightly smaller than that of the perfluoro chain; however the smaller alkoxy cross-section is compensated for partly by different non-planar conformations of which the one shown in Figs 3d and 4d is an example. The fact that the cross-sectional profile $A(x)$ in Figs 3c and 4c is still relatively uneven may not be a serious problem in reality since it would be at least partially ironed out by (a) a variety of conformations with increasingly tilted non-fluorinated end-section, and (b) by longitudinal translational disorder, i.e. the McMillan order parameter being less than 1. The important point to note is that the relative fluctuation (unevenness) in $\rho(x)$ (Figs 3c and 4c) is larger than that in $A(x)$; hence ironing out the former still leaves fluctuations in the latter, thus maintaining the source of diffraction.

Further evidence in favour of the interdigitated structure of smectic esters is provided by the comparison between the reconstructed $\Delta\rho(x)$ curves for the two compounds. The two curves differ only in the width of the central maximum. This is entirely consistent with the model where the two smectic structures differ only by the length of their interdigitated high-ρ perfluorinated segments. With the number of X-ray reflections as limited as in liquid crystals, such "isomorphous replacement" methods, where molecular structure is varied in a systematic way, are proving very valuable in structure determination [15].

Additional information on molecular arrangement is contained in the magnitude of the combined intensitiey of the low-angle (layer) reflections. It is evident that $\sum_{n=1}^{3} I_n$ is significantly lower in **12F8PhCO_2H** than in the two esters. Although absolute intensities were not measured, for a comparison between samples the area under the diffuse wide-angle scattering peak can be taken as normalization reference to a good approximation, since elemental compositions of the three compounds are very similar. One property of the scattering function, frequently used in low-angle studies, is that, irrespective of how the scattered intensity is distributed over the reciprocal space, the total scattered intensity per unit volume of the specimen is determined entirely by the mean square electron density fluctuation in the sample, $\langle \Delta\rho^2 \rangle$:

$$\int_0^\infty I(Q)Q^2\,\mathrm{d}Q \cong \int_0^\infty I_{\mathrm{Lor}}(Q)\,\mathrm{d}Q \propto \langle \Delta\rho^2 \rangle$$

where I_{Lor} is Lorentz corrected intensity. The fact that $\sum_{n=1}^{3} I_n$ is lower for the acid compared with the esters confirms that its electron density profile is smoother (Fig. 5b) than those of the esters (Figs 3b and 4b).

One can speculate about the cause of the observed difference in molecular packing between the esters and the acid. The latter has a strong tendency to form hydrogen-bonded dimers, hence the double layer formation is not unexpected; similar structures are found in both crystalline and liquid crystalline alkoxybenzoic acids [16, 17]. Pairing of benzoic groups requires their collinear orientation, which imposes a constraint on the rest of the molecule. Such constraint does not apply to esters which do not hydrogen-bond, hence other packing considerations prevail.

It is worth noting that alkoxybenzoic acids form smectic liquid crystals also without fluorination, because they contain the extended, comparatively rigid, H-bonded aromatic dimer core. Alkoxybenzoate esters, on the other hand, lack an extended rigid core and hence do not form liquid crystals. The polyphilic nature of the present ester compounds **$\mathbf{10F6PhCO_2CH_3}$** and **$\mathbf{12F8PhCO_2CH_3}$**, brought about by perfluorination of a part of the chain, therefore holds the key to their mesogenic property.

According to the present model of the smectic phase in **$\mathbf{10F6PhCO_2H}$**, this should be regarded as S_C. This assignment could not be made solely on the basis of optical birefringence texture or X-ray spacing. It should be pointed out here that a small endotherm can be noted at 190°C, close to the isotropisation endotherm; this high-temperature phase has been tentatively designated as S_A [9]. The temperature range of this phase was too narrow for reliable identification by X-ray diffraction.

5. Conclusion

Polyphilic partially perfluorinated alkoxybenzoate esters and alkoxybenzoic acid display smectic phases whose structures were studied by X-ray diffraction and modelling. The method whereby 1-dimensional electron density profiles reconstructed from diffraction intensities are matched to those calculated from structural models, has proven useful in both determining molecular arrangement in the smectic phase and in phase identification. An S_{Ad} phase is found in esters **$\mathbf{10F6PhCO_2CH_3}$** and **$\mathbf{12F8PhCO_2CH_3}$**, with interdigitated perfluorinated alkyl segments. In contrast, a double-layer S_C phase, sometimes denoted S_{C2}, is found in the acid **$\mathbf{10F6PhCO_2H}$**. In the absence of global orientation this information could have not been obtained by other methods, particularly as birefringence textures were ambiguous. The procedure used here is particularly suitable to polyphilic liquid crystals which are characterized by a complex electron density profile and a high translational order parameter.

Acknowledgement

We wish to thank Professor D. A. Dunmur for his active interest in this work and for helpful discussions and guidance.

References

1. A. SKOULIOS and D. GUILLON, *Mol. Cryst. Liq. Cryst.* **165** (1988) 317.
2. F. G. TOURNILHAC, L. M. BLINOV, J. SIMON and S. V. YABLONSKY, *Nature* **359** (1992) 621.
3. F. G. TOURNILHAC, L. BOSIO, J. SIMON, L. M. BLINOV and S. V. YABLONSKY, *Liq. Cryst.* **14** (1993) 405.
4. J. PROST, R. BRUINSMA and F. TOURNILHAC, *J. Phys. II (France)* **4** (1994) 169.
5. J. W. GOODBY, *J. Mater. Chem.* **1** (1991) 307.
6. A. FUKUDA, Y. TAKANISHI, T. ISOZAKI, K. ISHIKAWA and H. TAKEZOE, *J. Mater. Chem.* **4** (1994) 997.
7. F. TOURNILHAC, L. BOSIO, J. F. NICOUD and J. SIMON, *Chem. Phys. Lett.* **145** (1988) 452.
8. K. NOBLE and D. A. DUNMUR, unpublished.
9. G. JOHANSSON, V. PERCEC, G. UNGAR and K. SMITH, *Chem. Mater.* **9** (1997) 164.
10. V. PERCEC, G. JOHANSSON, G. UNGAR and J. ZHOU, *J. Amer. Chem. Soc.* **118** (1996) 9855.
11. V. S. K. BALAGURUSAMY, G. UNGAR, V. PERCEC and G. JOHANSSON, *ibid.* **119** (1997) 1539.
12. R. M. RICHARDSON, A. J. LEADBETTER, M. A. MAZID and P. A. TUCKER, *Mol. Cryst. Liq. Cryst.* **149** (1987) 329.
13. L. M. BLINOV, T. A. LOBKO, B. I. OSTROVSKII, S. N. SULIANOV and F. G. TOURNILHAC, *J. Phys. II (France)* **3** (1993) 1121.
14. G. UNGAR, V. PERCEC and R. RODENHOUSE, *Macromolecules* **24** (1991) 1996.
15. G. UNGAR, V. PERCEC, M. N. HOLERCA, G. JOHANSSON and J. A. HECK, *Chem. Eur. J.*, to appear.
16. R. F. BRYAN, P. HARTLEY, R. W. MILLER and M. S. SHEN, *Mol. Cryst. Liq. Cryst.* **62** (1980) 281.
17. R. F. BRYAN, P. HARTLEY and R. W. MILLER, *ibid.* **62** (1980) 311.

Received 10 March
and accepted 14 March 2000